Institute of Paper Science and Technology
Atlanta, Georgia

IPST TECHNICAL PAPER SERIES

NUMBER 448

THE DISTRIBUTION OF PERFORATIONS IN A RADIALLY THINNING LIQUID SHEET

T.M. SPIELBAUER AND C.K. AIDUN

JULY 1992

The Distribution of Perforations in a Radially Thinning Liquid Sheet

T.M. Spielbauer and C.K. Aidun

Submitted to
TAPPI 1992 Engineering Conference
September 14–17, 1992
Boston, Massachusetts

THE DISTRIBUTION OF PERFORATIONS IN A RADIALLY THINNING LIQUID SHEET

T.M. Spielbauer
Graduate Student
IPST
Atlanta, GA
USA

C.K. Aidun
Asst. Professor
IPST
Atlanta, GA
USA
(404) 853-9777
(404) 853-9510 (FAX)

ABSTRACT

This investigation of sprays is focused on the formation and breakup of sheets formed by splash plate nozzles. An expression for predicting the thickness of a sheet spreading on a plate was obtained by modifying equations available in the literature. This sheet thickness predicted with this expression correlates well with measurements made during this study; thus this equation may be a useful tool in the design of splash plate nozzles.

High speed video images of splash plate sheets were collected at a series of downstream locations. The perforations observed were counted, and the data were used to determine the radial distribution of perforations as a function of the nozzle orifice diameter and the jet velocity. For each combination of orifice diameter and jet velocity, there was a critical distance downstream at which rapid perforation occurred.

The predicted thickness at the plate edge was then used as a basis for estimating the thickness of the free sheet, downstream from the plate edge. The perforation counts are plotted versus the calculated downstream sheet thickness, and the majority of the perforations are shown to be formed in a narrow range of sheet thicknesses.

KEYWORDS: Fluid dynamics, Fluid flow, Fluid mechanics, Hydrodynamics, Liquids, Nozzles, Perforations, Sheets, Spraying, Thickness, Velocity, Waves

INTRODUCTION

Spraying converts a bulk quantity of liquid into a large number of small drops. Such a transformation is useful in many operations including: liquid fuel injection, spray drying, pesticide application, spray painting, and metal powder manufacture.[1] In processes such as fuel injection and spray drying, the formation of drops increases the surface area per unit volume of liquid and thus enhances energy and mass transfer rates.[2,3]

The introduction of black liquor into the combustion zone of a recovery boiler is a spray application of particular importance in the pulp and paper industry. A number of different nozzles are used to deliver the liquor including splash plate, swirl cone, and fan spray designs. Each of these devices produces a radially thinning liquid sheet as an intermediate step in the reservoir. The circuit is closed when the micrometer tip touches the top surface of the splash plate. This point is used as the reference position. The micrometer tips are retracted until they just touch the top surface of the liquid flowing across the plate. The location of the top sheet surface relative to the reference position is taken to be the thickness of the sheet.

A summary of the range of operating conditions investigated is given in Table 3. Included in this table is the maximum value of r_t calculated for each nozzle. (See Eq. 10.) In all cases, the thickness probes were in the fully developed boundary layer region; therefore, the measured sheet thicknesses should be given by Eq. 14, and the sheet thickness ratio should be given by Eq. 18.

Table 3. Range of operating conditions investigated in the sheet thickness studies.

nozzle style	d_0 (mm)	number of trials	velocity (m/s)	viscosity (cp)	density (kg/m^3)	Reynold's Number	maximum r_t (cm)
#1	4.66	18	8.6-24.9	69-85	1220	900-3200	1.1
#6	6.36	21	5.9-17.2	51-67	1210	1300-4400	1.6
#4	6.56	14	5.6-18.3	79-102	1220	700-2500	1.4
#5	8.45	17	3.0-12.6	85-96	1220	500-2400	1.8

The sheet thicknesses measured by each of the three probes were used to calculate an average sheet thickness and the standard deviation of the probe measurements. The normalized standard deviation (the standard deviation divided by the average sheet thickness) varied from one to 20 percent, with an average value of six percent.

For each trial, the average sheet thickness was divided by the theoretical inviscid sheet thickness calculated from Eq. 7. The resulting experimental sheet thickness ratio is plotted versus $\frac{1}{Re}\left(\frac{x}{d_0}\right)^3$ in Fig. 7. The theoretical curve based upon the boundary layer velocity profile in the fully-developed region is shown as a solid line. The best fit regression line, shown as a dashed line, is given by

$$\frac{H(r)}{H_{id}(r)} = [1.55 \pm 0.08] + \frac{[40.2 \pm 1.4]}{Re_{jet}}\left(\frac{r}{d_0}\right)^3, \qquad (19)$$

with a coefficient of determination of 0.978.

The measured slope agrees, within the uncertainty limits at the 95% confidence level, to the value predicted using the fully-developed boundary layer results. The intercepts do not agree, and the reduction in sheet velocity and the corresponding increase in sheet thickness are under-predicted at all jet velocities. The magnitude of this difference ranged from 5% to 9%, decreasing with increasing values of $(1/Re)(x/d_0)^3$.

Downstream Sheet Thickness

Once the liquid leaves the plate to form a free, radially thinning sheet, viscous forces will no longer decrease its velocity, and the sheet velocity is assumed to be equal to the average sheet velocity at the plate edge. Thus, if the thickness of the sheet at the plate edge is known, then the downstream thickness of the sheet can be calculated from a simple mass balance given by

$$2\pi r_p H(r_p) U_{avg}(r_p) \rho_{liq} = 2\pi r H(r) U_{avg}(r_p) \rho_{liq}, \tag{20}$$

where the subscript p denotes the value of a parameter at the edge of the plate. Upon rearrangement the downstream sheet thickness can be written as

$$H(r) = \frac{r_p H(r_p)}{r}, \qquad \text{for } r > r_p. \tag{21}$$

The operating conditions for each perforation count experiment were used in conjunction with Eq. 19 to calculate the sheet thickness at the edge of the splash plate (r_p= 2.54 cm). Equation 21 was then used to calculate the thickness of the sheet at the center of each imaging area.

The perforations counts, previously plotted versus the distance downstream and jet velocity, are now replotted versus the calculated downstream sheet thickness, as shown in Fig. 8. Six additional experiments were performed in which the perforations were too numerous to count. Many of the images collected during these trials showed clumps, strands, and drops of liquid. The range of sheet thicknesses calculated for these six trials is labeled the breakup region in Fig. 8.

The number of perforations formed per centimeter of radial span appears to increase rapidly when the sheet thickness is reduced to about 70 microns. The breakup of the sheet into the clumps and strands which precede drop formation is completed before the calculated sheet thickness is reduced below 50-60 microns.

DISCUSSION

Experimental sheet thickness data, obtained using extended micrometer probes, were used to test our ability to predict the downstream sheet thickness on the plate of a simple splash plate nozzle using expressions originally derived by Watson.[9] The linear relationship between the downstream sheet thickness and $\frac{1}{Re}\left(\frac{x}{d_0}\right)^3$ was confirmed; however, the sheet thickness was underpredicted by an average of 7.3%. This difference between the measured and predicted thickness is believed to be the result of neglecting momentum losses which occur in the region of jet impact.

Despite the difference between the predicted and measured values of the sheet thickness ratio, the expression derived should be useful for predicting the effects of the fluid properties, the jet diameter, and the jet velocity on the downstream sheet thickness and velocity. It should be noted that only the expression obtained for the fully-developed boundary layer region ($r > r_L$) was confirmed experimentally, while the geometry of some splash plate nozzles may require the use of the developing boundary layer equation.

The equation for the sheet thickness ratio in the fully-developed boundary layer region can be rearranged to obtain

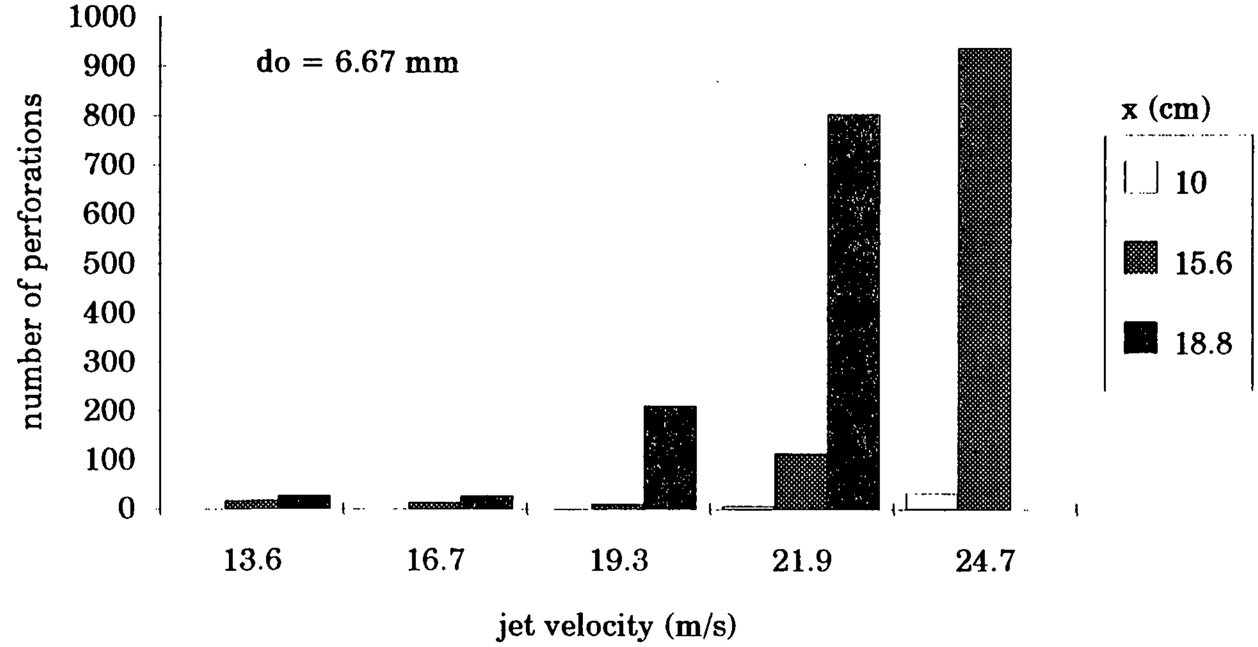

1000
900
800
700
600
500
400
300
200
100
0
number of perforations
do = 6.67 mm
x (cm)
10
15.6
18.8
13.6
16.7
19.3
21.9
24.7
jet velocity (m/s)

Fig. 5.

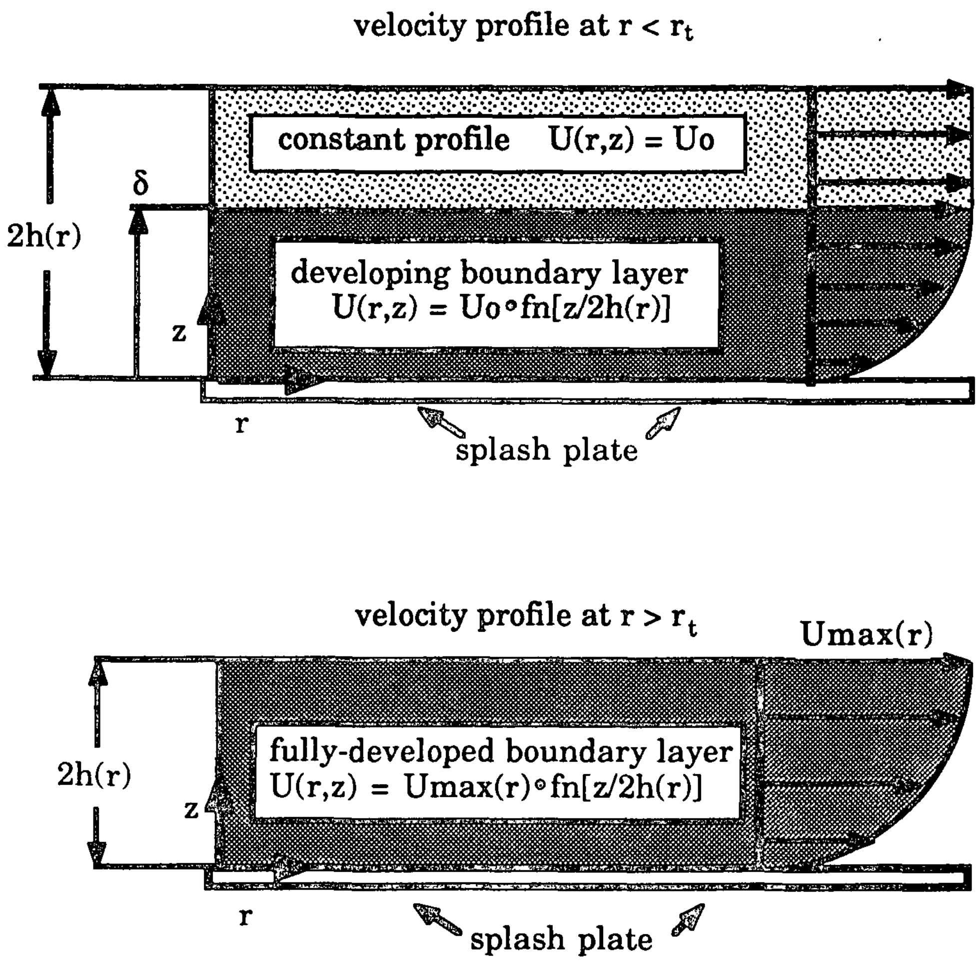

velocity profile at r < rt
constant profile U(r,z) = Uo
δ
2h(r)
developing boundary layer
U(r,z) = Uo∘fn[z/2h(r)]
z
r
splash plate
velocity profile at r > rt
Umax(r)
fully-developed boundary layer
U(r,z) = Umax(r)∘fn[z/2h(r)]
2h(r)
z
r
splash plate

Fig. 6.

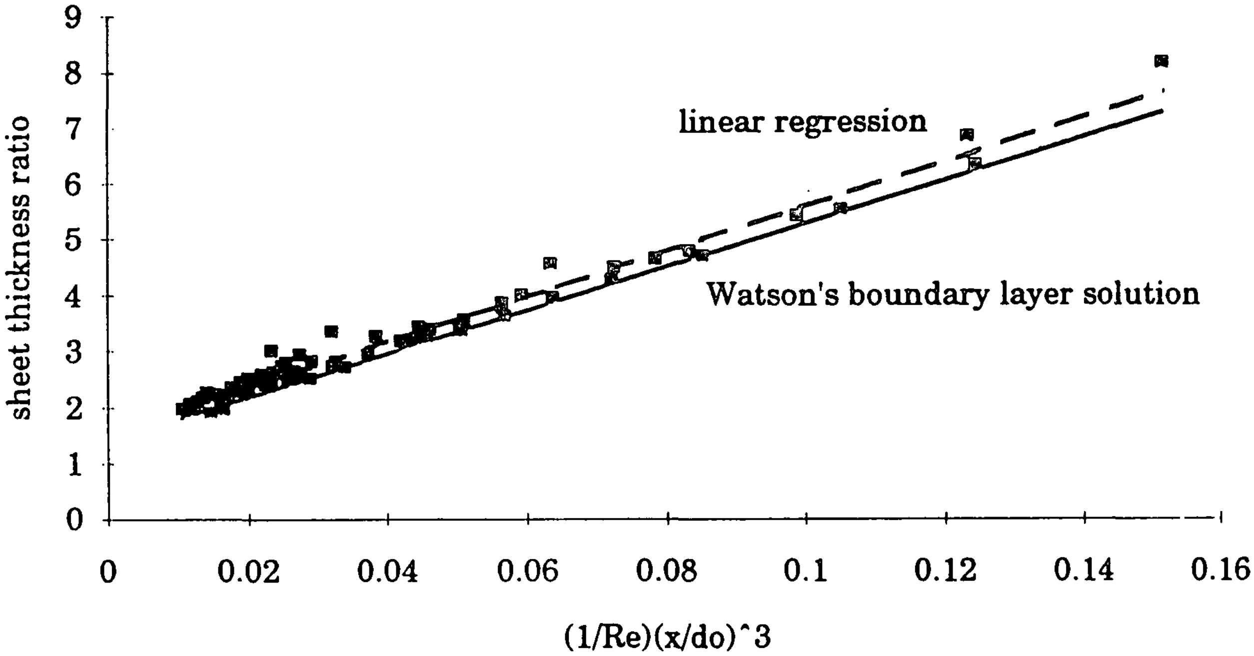
sheet thickness ratio
9
8
7
6
5
4
3
2
1
0
0
0.02
0.04
0.06
0.08
0.1
0.12
0.14
0.16
(1/Re)(x/do)^3
linear regression
Watson's boundary layer solution

Fig. 7.

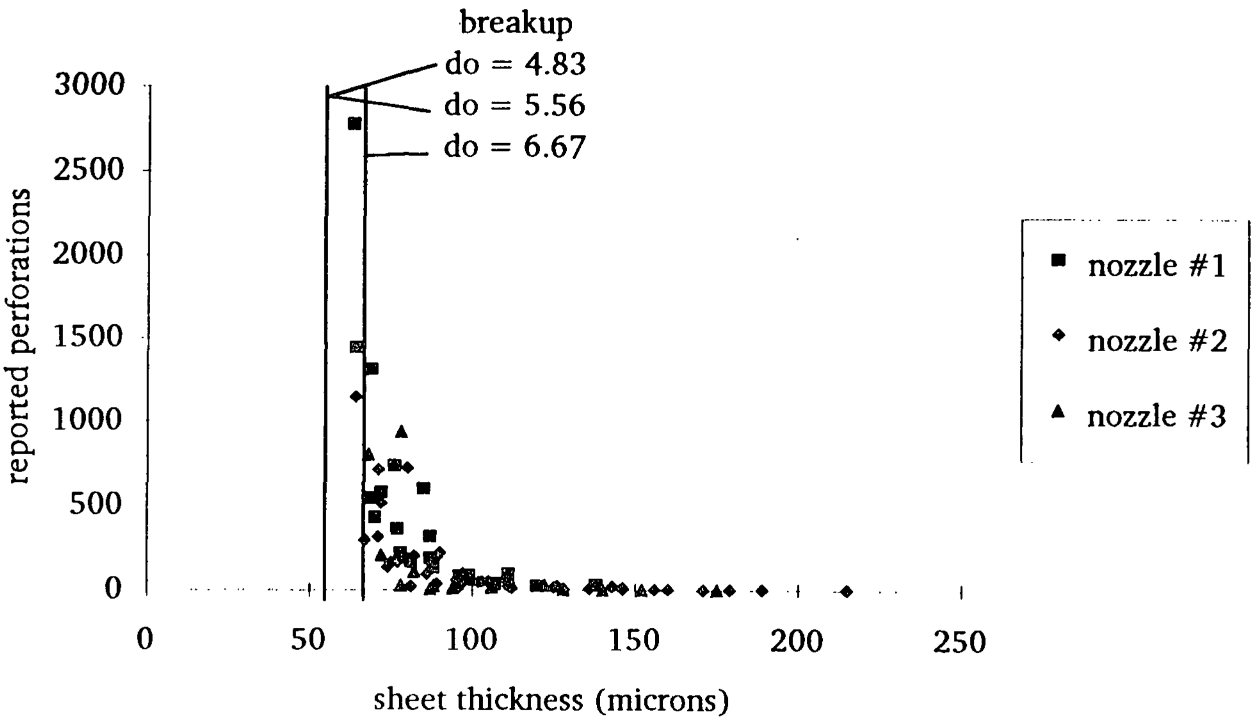

breakup
do = 4.83
do = 5.56
do = 6.67
3000
2500
2000
1500
1000
500
0
reported perforations
0
50
100
150
200
250
sheet thickness (microns)
nozzle #1
nozzle #2
nozzle #3

Fig. 8.